Noise on resistive switching: A Fokker-Planck approach

G. A. Patterson

Instituto Tecnológico de Buenos Aires, Ciudad de Buenos Aires, Argentina‡

E-mail: gpatters@itba.edu.ar

D. F. Grosz

Instituto Balseiro, San Carlos de Bariloche, Argentina
Consejo Nacional de Investigaciones Científicas y Técnicas, Argentina

E-mail: grosz@ib.edu.ar

P. I. Fierens

E-mail: pfierens@itba.edu.ar
Instituto Tecnológico de Buenos Aires, Ciudad de Buenos Aires, Argentina
Consejo Nacional de Investigaciones Científicas y Técnicas, Argentina

September 2015

Abstract. We study the effect of internal and external noise in the phenomenon of resistive switching. We consider a non-harmonic external driving signal and provide a theoretical framework to explain the observed behavior in terms of the related Fokker-Planck equations. It is found that internal noise causes an enhancement of the resistive contrast and that noise proves to be advantageous when considering short driving pulses. In the case of external noise, however, noise only has the effect of degrading the resistive contrast. Furthermore, we find a relationship between the noise amplitude and the driving signal pulsewidth that constrains the persistence of the resistive state. In particular, results suggest that strong and short driving pulses favor a longer persistence time, an observation that may find applications in the field of high-integration high-speed resistive memory devices.

Keywords: Memristor, Noise, Fokker-Planck Submitted to: *J. Stat. Mech.*

‡ Now at Departament d'Enginyeria Electrònica, Universitat Autònoma de Barcelona, Barcelona, Spain

1. Introduction

In recent years, several technologies have emerged as candidates to replace the current generation of non-volatile memories. A promising technology, known as resistive RAMs (RRAMs), relies on the storage of digital data on distinct resistive states, and is based on the phenomenon of resistive switching, i.e., the ability displayed by certain materials to switch between resistive states when subjected to an external electric field. Such behavior provides a physical realization of a memristor, first introduced by Chua [1]. The potential application of resistive switching to high-density information storage motivates the investigation of the influence of noise in such devices. Stotland and Di Ventra were the first authors to present an analysis of the influence of noise on memristors [2] and ensuing work by our group further explored the interplay between noise and resistive switching [3, 4, 5]. In Ref. [2] the influence of additive white Gaussian noise on a simple model of a memristor put forth by Strukov *et al.* [6] was studied. By means of numerical simulations, it was shown that the contrast between low- and high-resistive states is enhanced by the addition of internal noise when a weak harmonic driving signal is applied, and an explanation of the observed phenomenon in terms of stochastic resonance was provided. In this paper, we go back to the work by Stotland and Di Ventra and extend it in several directions. First, motivated by the application of resistive switching for resistive RAMs, we consider a non-harmonic external (pulsed) driving signal and provide a theoretical explanation of the observed behavior in terms of the related Fokker-Planck (FP) equation. Then, we consider the case of external noise, *i.e.*, noise added to a weak driving signal, a case of practical interest as it deals with fluctuating and/or noisy driving signals , where we also propose a qualitative model in terms of the corresponding FP equation.

2. A simple model of memristor

According to the model by Strukov *et al.* [6], resistance in a memristor can be written as

$$R(x) = \alpha(1 - \delta R\, x), \tag{1}$$

where $\alpha, \delta R \in \mathbb{R}^+$ are constants and $x \in [0, 1]$ is a state variable governed by the equation

$$\frac{dx}{d\tau} = \frac{4x(1-x)}{1 - \delta R\, x} v(\tau), \tag{2}$$

where τ is a suitably normalized time variable and $v(\tau)$ is the (normalized) external driving voltage. Integrating equation 2 we find that

$$\frac{x(\tau)}{(1 - x(\tau))^{1/\beta}} = g(\tau), \tag{3}$$

where $\beta = (1 - \delta R)^{-1}$ and

$$g(\tau) = \frac{x(0)}{(1 - x(0))^{1/\beta}} \exp\left\{4 \int_0^\tau v(t)dt\right\}. \tag{4}$$

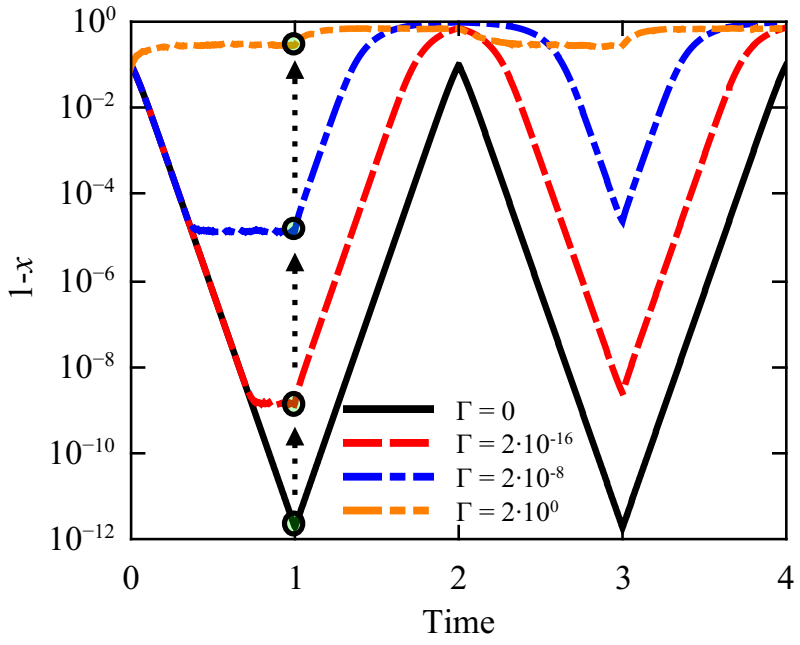

Figure 1. Temporal evolution of the state variable x for several noise intensities. Results from the average of 1000 noise realizations.

Hence, $x(\tau)$ can be found as a solution to the equation

$$x^{\beta}(\tau) + g^{\beta}(\tau)x(\tau) - g^{\beta}(\tau) = 0, \tag{5}$$

In Ref. [7], Cai *et al.* present an analytical study of the behavior of the state variable x. Biolek *et al.* [8] also derive an explicit expression for the resistance. In our case, we only need to point out the dependence of the solution on the initial condition $x(0)$.

3. Internal noise

In this section, we consider the case in which equation (2) is modified by additive white Gaussian noise $\eta(\tau)$ such that $\langle \eta(\tau) \rangle = 0$ and $\langle \eta(\tau)\eta(\tau') \rangle = \Gamma\delta(\tau - \tau')$. Furthermore, we consider a non-harmonic drive $v(\tau)$ consisting of a sequence $+1 \to -1 \to +1 \to \cdots$ pulses of width τ_b.

Fig. 1 shows the temporal evolution of x for several noise intensities, $\tau_b = 1$, and $\delta R = 3/4$. Observe that the maximum value that the state variable x reaches after a $+1$ pulse is applied decreases as the noise intensity increases, as noted by circles and arrows. A usual way of quantifying the contrast between low (R_l) and high (R_h) resistance states is through the Electric Pulse Induced Resistance (EPIR) ratio given by $\frac{R_h - R_l}{R_l}$. As it can be observed in Fig. 2, for certain pulse durations, the EPIR ratio is maximized at a certain noise intensity .

Results in Fig. 1 can be understood by resorting to the related Fokker-Planck

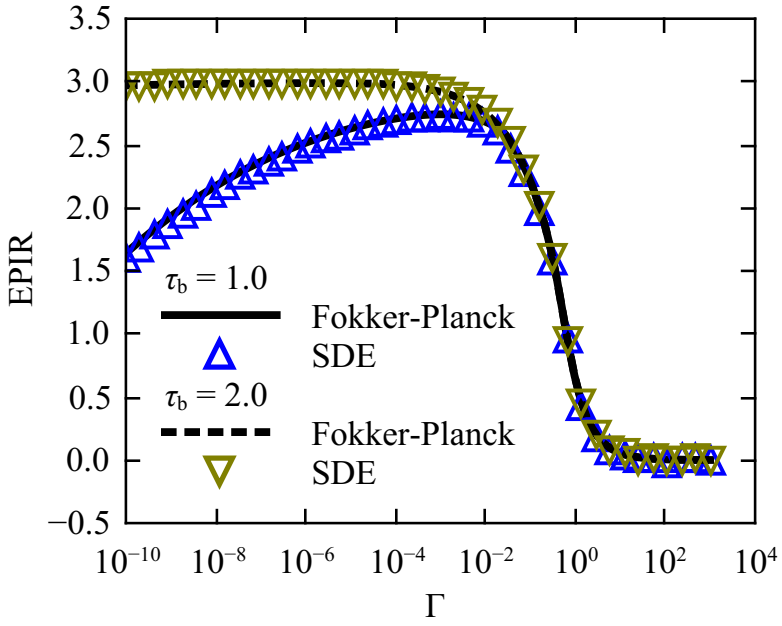

Figure 2. EPIR ratio *vs.* internal noise intensity. Solid and dashed lines correspond to quasi-analytic predictions developed in the text. Results corresponding to the average of 1000 realizations of the stochastic differential equation are represented by triangles.

equation

$$\frac{\partial P}{\partial \tau} = -\frac{\partial}{\partial x}\left\{\frac{4x(1-x)}{1-\delta R\, x} v(\tau) P(x,\tau)\right\} + \frac{\Gamma}{2}\frac{\partial^2}{\partial x^2} P(x,\tau). \tag{6}$$

Assuming that τ_b is large enough, we can work with the stationary solution to this equation, *i.e.*, $P(x,\tau_b) \approx P_s(x)$. From equation 6 it follows that

$$\frac{\partial^2}{\partial x^2} P_s(x) = \frac{\partial}{\partial x}\left\{\frac{2}{\Gamma}\frac{4x(1-x)}{1-\delta R\, x} v(\tau_b^-) P_s(x)\right\} \tag{7}$$

Integrating once,

$$\frac{\partial P_s}{\partial x} - \left.\frac{\partial P_s}{\partial x}\right|_{x=0} = \frac{2}{\Gamma}\frac{4x(1-x)}{1-\delta R\, x} v(\tau_b^-) P_s(x), \tag{8}$$

where we have assumed that the right-hand side is zero at $x = 0$ (*i.e.*, $\lim_{x\to 0} x P_s(x) = 0$). Since x is constrained to the interval $[0,1]$, we assume reflecting barriers at the borders of the interval and, hence, $\left.\frac{\partial P_s}{\partial x}\right|_{x=0} = \left.\frac{\partial P_s}{\partial x}\right|_{x=1} = 0$. We obtain

$$P_s(x) \propto \exp\left\{\frac{2}{\Gamma}\int_0^x v(\tau_b^-)\frac{4y(1-y)}{1-\delta R y} dy\right\}, \tag{9}$$

where $\langle x(\tau_b)\rangle$ can be computed by numerical integration. Fig. 3 shows a good agreement between simulations of the stochastic differential equation and results obtained through the stationarity hypothesis. As it is readily seen from equations (3)-(5), the deterministic evolution of $x(\tau)$ depends strongly on the initial condition. One of the effects of noise is to erase the memory of the initial condition. Indeed, as expected, the stationary probability distribution in equation (9) does not depend on the initial condition.

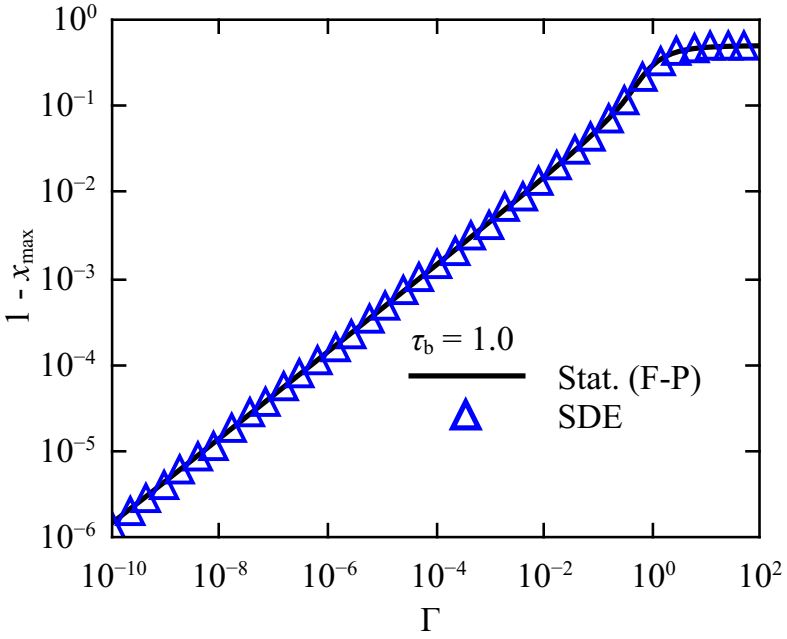

Figure 3. Maximum value of x vs. noise intensity: approximation given by the stationary distribution (solid line) and by integration of the stochastic differential equation (blue triangles).

However, the time required to achieve a stationary condition does depend on the initial condition (first term in equation (6)). In general, such convergence time decreases as the noise intensity increases, *i.e.*, a higher noise intensity erases the memory of the initial condition faster.

We can try to use the stationary hypothesis to compute the minimum value attained by x after a -1 pulse is applied, *i.e.*, $x(2\tau_b)$. Fig. 4 shows $\langle x(2\tau_b)\rangle$ as a function of the noise intensity (the stationary probability is similar to that in equation (9)). The behaviour for low noise intensities deviates from that predicted by the stationary distribution. Indeed, for the given initial condition ($\langle x(\tau_b)\rangle$ in Fig. 3, the value of x at the end of the previous $+1$ pulse), the pulse duration τ_b is not long enough to allow for the convergence to stationarity and higher noise intensities are needed to erase the memory of the initial condition. Moreover, when the noise intensity is low, the value of $x(2\tau_b)$ can be approximated by the deterministic solution in equations (3)-(5).

Using the predictions based on the stationary probability distribution and the deterministic solution (for low noise intensities) in Figs. 3-4, we can estimate the EPIR ratio. The result is shown in Fig. 2 and agrees very well with simulations. Intuitively, the main effect of the added noise is to lower the value of x at the end of the first $+1$ pulse in such a way that $\langle x(\tau_b)\rangle$ is smaller than that expected from the deterministic solution. For low noise intensities, this 'new' initial condition for the differential equation for $\tau > \tau_b$ results in a mean value of $x(2\tau_b)$ smaller than that in the noiseless case and, thus leads to an enhanced EPIR ratio. For high noise intensities, the values of the state variable x attained at the end of each pulse are independent of the initial conditions

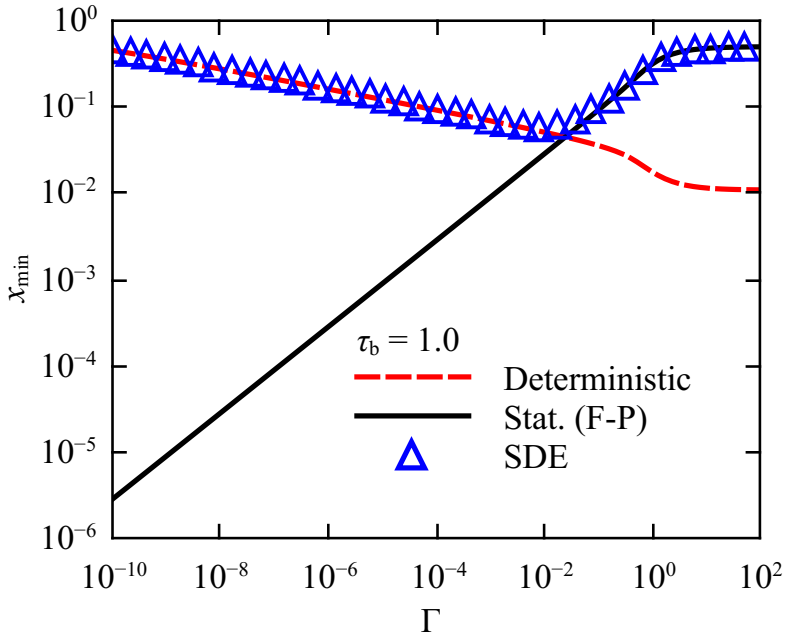

Figure 4. Minimum value of x vs. noise intensity: approximation given by the stationary distribution (solid line), approximation given by the deterministic solution (dashed), and result of integrating the stochastic differential equation (blue triangles).

and determined by the stationary solution of the corresponding Fokker-Planck equation. Furthermore, as Γ increases, the distribution in equation (9) broadens, $\langle x_s \rangle$ tends to 1/2 and the EPIR ratio approaches to zero.

Let us now return to Eqs. 8-9. From equation 8, it is easy to see that $P_s(x)$ is increasing (decreasing) when $v(\tau_b^-) > 0$ (< 0). Thus, $P_s(x)$ attains its maximum at $x = 1$ when a positive input is applied, and at $x = 0$ when the input voltage is negative. Evaluating the integral in the exponent of equation 9, we find

$$P_s(x) \propto \exp\left\{\frac{8v(\tau_b^-)}{\Gamma}\left[\frac{\delta R x\,(\delta R x - 2\delta R + 2) - 2\,(1-\delta R)\log\,(1-\delta R x)}{2(\delta R)^3}\right]\right\}. \tag{10}$$

Although this expression is not very complex, we can get a better intuition by assuming that $\delta R \ll 1$. In this case, $\log(1-\delta R\,x) \approx -\delta R\,x$ and

$$P_s(x) \approx \mathcal{N} \exp\left\{\frac{\left[x + 2\left(\frac{1}{\delta R} - 1\right)\right]^2}{\frac{\Gamma \delta R}{4v(\tau_b^-)}}\right\}, \tag{11}$$

where $\mathcal{N}$ is a normalizing constant. From this expression, it is easy to see that the stationary distribution is almost uniform when $\frac{\Gamma\delta R}{4|v(\tau_b^-)|} \gg 1$, and that it peaks at the extremes of the interval when $\frac{\Gamma\delta R}{4|v(\tau_b^-)|} \ll 1$. Although one may expect for the dispersion of the distribution to depend on the ratio $\Gamma/|v(\tau_b^-)|$, we find the influence of δR to be nontrivial. Indeed, it is as if the noise intensity, measured by Γ, is effectively scaled by δR. Since δR is a measure of the highest possible contrast between the low- and high-resistance states of the memristor, we must conclude that a higher contrast leads to a high uncertainty on the resistance attained under the influence of internal noise.

Let us now consider the opposite case where $\delta R \approx 1$. Under this condition, it is easy to see that

$$P_s(x) \approx \mathcal{N} \exp\left\{ \frac{x^2}{\frac{\Gamma}{4v(\tau_b^-)}} \right\}, \tag{12}$$

It is also simple to compute approximations to the expected value of x in this case, and obtain

$$\langle x_s \rangle \approx \mathcal{N} \frac{\Gamma}{8v(\tau_b^-)} \left[\exp\left\{ \frac{4v(\tau_b^-)}{\Gamma} \right\} - 1 \right]. \tag{13}$$

Substituting this result into equation 1, we can estimate the EPIR ratio when τ_b is large as follows

$$\begin{aligned} \langle \text{EPIR} \rangle &\approx \frac{R(\langle x_s^- \rangle) - R(\langle x_s^+ \rangle)}{R(\langle x_s^+ \rangle)} = \frac{\langle x_s^+ \rangle - \langle x_s^- \rangle}{1 - \langle x_s^+ \rangle} \\ &\approx \frac{\Gamma}{8|v(\tau_b^-)|} \frac{\mathcal{N}^+ \mathrm{e}^{\frac{4|v(\tau_b^-)|}{\Gamma}} + \mathcal{N}^- e^{-\frac{4|v(\tau_b^-)|}{\Gamma}} - \mathcal{N}^+ - \mathcal{N}^-}{1 - \frac{\mathcal{N}^+ \Gamma}{8|v(\tau_b^-)|} \left[e^{\frac{4|v(\tau_b^-)|}{\Gamma}} - 1 \right]}, \end{aligned}$$

where the superscript + (−) denotes the stationary values when the input voltage is positive (negative). When Γ is large, the distribution is almost uniform and $\mathcal{N} \approx 1$. Therefore,

$$\begin{aligned} \langle \text{EPIR} \rangle &\approx \frac{\Gamma}{4|v(\tau_b^-)|} \frac{\cosh\left(\frac{4|v(\tau_b^-)|}{\Gamma} \right) - 1}{1 - \frac{\Gamma}{8|v(\tau_b^-)|} \left[\exp\left\{ \frac{4|v(\tau_b^-)|}{\Gamma} \right\} - 1 \right]} \\ &\approx \frac{\Gamma}{4|v(\tau_b^-)|} \frac{\frac{1}{2}\left(\frac{4|v(\tau_b^-)|}{\Gamma} \right)^2}{1 - \frac{\Gamma}{8|v(\tau_b^-)|} \left(\frac{4|v(\tau_b^-)|}{\Gamma} \right)} \approx \frac{|v(\tau_b^-)|}{\Gamma}. \end{aligned} \tag{14}$$

As expected, the EPIR ratio decreases with increasing noise intensity. This behavior agrees qualitatively with results presented in Fig. 2. However, in the preceding equations, the EPIR ratio increases unbounded with decreasing Γ as a consequence of having assumed $\delta R = 1$. When $\delta R < 1$, it is readily seen that the maximum EPIR ratio is $\delta R/(1 - \delta R)$ and this is the value observed in Fig. 2 for small Γ and $\tau_b = 2$. Summarizing, whenever the pulse length τ_b is long enough in order to assume that that stationary distributions are attained, no gain in the EPIR ratio can be obtained. However, if τ_b is shorter (e.g., $\tau_b = 1$ in Fig. 2), then there is an optimal noise intensity for which the EPIR ratio is maximized. From an application point of view, internal noise may be advantageously used to make faster memory devices based on resistive switching.

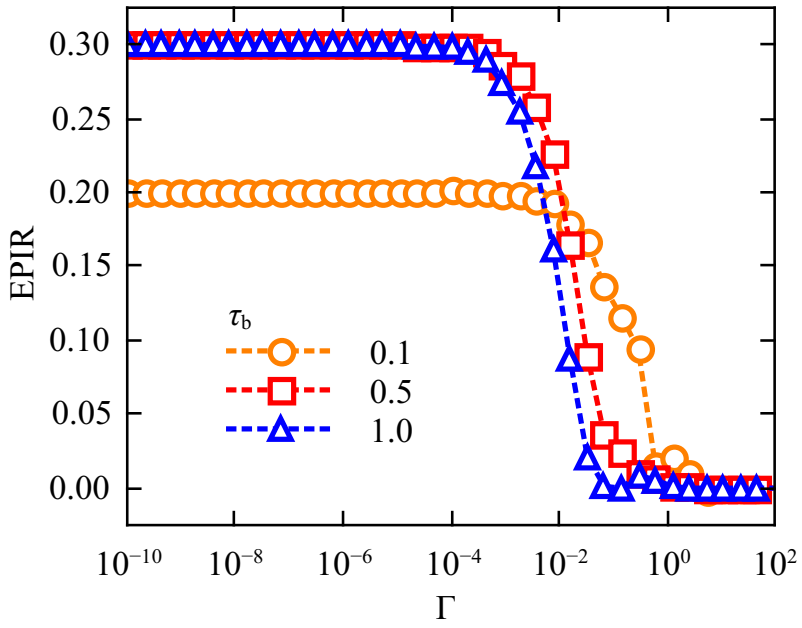

Figure 5. EPIR ratio as a function of external noise intensity. Results correspond to the average of 1000 realizations.

4. External noise

In this section we consider the case of external noise, *i.e.*, the case in which the state variable x is governed by the equation

$$\frac{dx}{d\tau} = \frac{4x(1-x)}{1-\delta R\, x}\left(v(\tau)+\eta(\tau)\right), \tag{15}$$

where $\eta(\tau)$ is white Gaussian noise as before. Fig. 5 shows the EPIR ratio as a function of noise intensity for several pulse widths ($x(0) = 0.9$). It is observed that there is no optimal noise intensity that maximizes the EPIR ratio.

An analytic expression for the probability distribution of $x(\tau)$ in equation 15 can be found. Indeed, it is easy to see that $x(\tau)$ in equation 15 must satisfy Eqs. 3 and 5 where $g(\tau)$ is re-defined as

$$g(\tau) = \frac{x(0)}{(1-x(0))^{1/\beta}} \exp\left\{4\int_0^\tau \left(v(t)+\eta(t)\right) dt\right\}. \tag{16}$$

Let us call $y(\tau)$ the integral in the exponential. From equation 3, we can write $y(\tau)$ as

$$y(\tau) = \log\left((1-x)^{-\frac{1}{4\beta}} x^{\frac{1}{4}}\right) - \log\left((1-x(0))^{-\frac{1}{4\beta}} x(0)^{\frac{1}{4}}\right).$$

If we call $F_{y(\tau)}$ and $F_{x(\tau)}$ the cumulative distribution functions of $y(\tau)$ and $x(\tau)$, respectively, then

$$F_{x(\tau)}(x) = F_{y(\tau)}\left(\log\left((1-x)^{-\frac{1}{4\beta}} x^{\frac{1}{4}}\right) - \log\left((1-x(0))^{-\frac{1}{4\beta}} x(0)^{\frac{1}{4}}\right)\right), \tag{17}$$

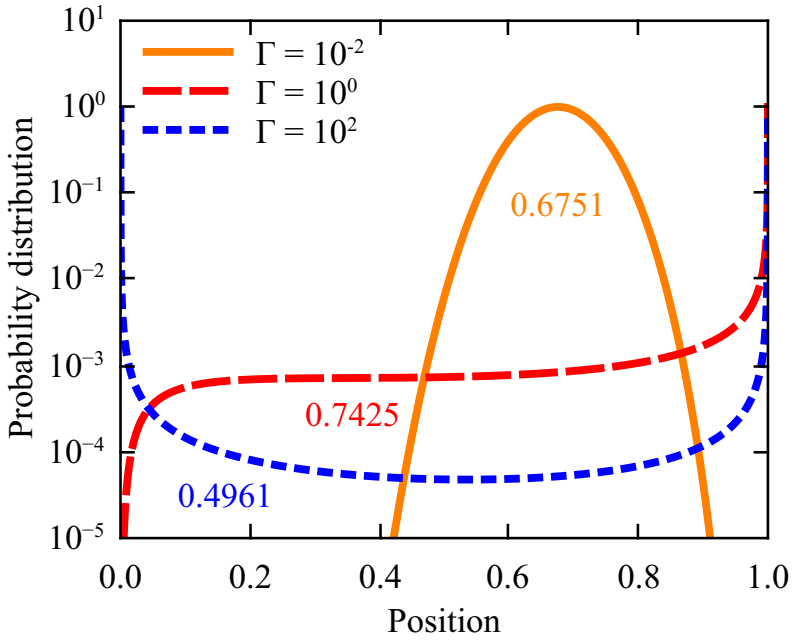

Figure 6. Probability distribution of $x(\tau_b)$ for several values of external noise intensity. The corresponding mean values are presented next to each distribution.

where we have assumed a deterministic initial condition $x(0)$. Taking the derivative with respect to x, we find

$$P(x,\tau) = P\left(\log\left[\left(\frac{1-x}{1-x(0)}\right)^{-\frac{1}{4\beta}}\left(\frac{x}{x(0)}\right)^{\frac{1}{4}}\right],\tau\right)\frac{1-\delta R\, x}{4x(1-x)}. \tag{18}$$

Figs. 6 and 7 show the probability distributions $x(\tau_b)$ (after the $+1$ pulse) and $x(2\tau_b)$ (after the -1 pulse), respectively. The initial condition is $x(0) = 0.5$, and parameter $\delta R = 3/4$. As expected, the distribution broadens as Γ increases. Moreover, for high noise intensities, $\langle x(\tau_b)\rangle \approx \langle x(2\tau_b)\rangle \approx 0.5$ and, therefore, the EPIR ratio is approximately zero. The behaviour of the EPIR ratio for other noise intensities can be understood by observing the distributions corresponding to $\Gamma = 1$ in Figs. 6 and 7. Note that, in this case, $\langle x(2\tau_b)\rangle \approx 0.7$. The state variable x does not 'return' to its initial condition $x(0) = 0.5$. The excursion of x values is smaller than that in the deterministic case and, thus, the EPIR ratio decreases.

Let us now go back to equation 18. The probability density function is a product of two factors. It is not difficult to see that, for all $\delta R \in (0,1)$, the second factor is a concave function for $x \in (0,1)$ and it grows unbounded when $x \to 0,1$. Therefore, if the density function has a maximum in that interval, it has to be provided by the first factor. However, when the product $\Gamma\tau$ is large, the first factor becomes nearly constant and, thus, we observe a bathtub shape for $\Gamma = 0.2$ in Figs. 6-7. Only when the product $\Gamma\tau$ is small, the influence of the first factor is relevant and the density exhibits a maximum roughly close to the position predicted by the deterministic Eqs. 3-5 (see the curves for $\Gamma = 0.01$ in Figs. 6-7). For intermediate values of $\Gamma\tau$, but τ large enough that

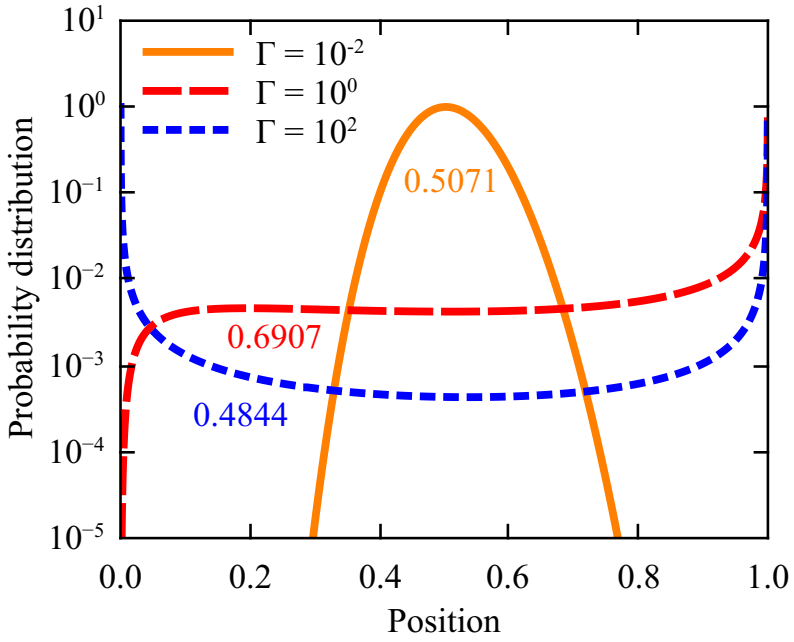

Figure 7. Probability distribution of $x(2\tau_b)$ *vs.* external noise intensity. The corresponding mean values are presented next to each distribution.

the deterministic predictions for $x(\tau)$ would be close to either 0 or 1, the decreasing tail behaviour of the first factor tends to compensate the growth of the second factor when x tends to 1 or 0, respectively. Indeed, this behaviour is observed for $\Gamma = 1$ in Figs. 6-7. From the application point of view, we may draw the conclusion that memory in a memristor is lost whenever $\Gamma\tau \gg 1$. In this sense, strong and short is more convenient than weak and long pulsing. Also, if external noise is present even in the absence of input, we can make a rough estimation of the memory persistence time as $T \sim \Gamma^{-1}$.

5. Conclusions

We introduced a Fokker-Planck approach to tackle the effect of internal and external noise on resistive switching. In the case of internal noise, we resorted to a Fokker-Planck approach to account for the enhancement of the resistive contrast found in numerical simulations with non-harmonic driving signals. In the context of resistive memory devices, results suggest that internal noise may be advantageous for short driving pulses, i.e., as it is the case of high-bandwidth devices. When exploring the effect of external noise, and by analyzing the probability density function of the state variable, we found that noise only has the effect of degrading the resistive contrast, and obtained a relationship between the noise amplitude and the pulsewidth of the driving signal that constrains the persistence of the resistive state. In particular, results suggest that strong and short driving pulses favor a longer persistence time, an observation that may find applications in the field of high-integration high-speed resistive memory devices.

Finally, it is important to point out that there exists evidence in the literature of external noise enhancing the resistive contrast [3, 4, 5]. It remains a matter of future work to explore whether it is possible to account for such an observation within the framework put forth in this paper.

Acknowledgments

We gratefully acknowledge financial support from ANPCyT under project PICT-2010 # 121.

References

[1] L. O. Chua. Memristor-the missing circuit element. *Circuit Theory, IEEE Transactions on*, 18(5):507–519, 1971.

[2] A. Stotland and M. Di Ventra. Stochastic memory: Memory enhancement due to noise. *Phys. Rev. E*, 85:011116, Jan 2012.

[3] G. A. Patterson, P. I. Fierens, A. A. García, and D. F. Grosz. Numerical and experimental study of stochastic resistive switching. *Phys. Rev. E*, 87:012128, Jan 2013.

[4] G. A. Patterson, P. I. Fierens, and D. F. Grosz. On the beneficial role of noise in resistive switching. *Applied Physics Letters*, 103(7):074102, 2013.

[5] G. A. Patterson, F. Sangiuliano Jimka, P. I. Fierens, and D. F. Grosz. Memristors under the influence of noise and temperature. *Physica Status Solidi (c)*, 12(1-2):187–191, 2015.

[6] D. B. Strukov, G. S. Snider, D. R. Stewart, and R. S. Williams. The missing memristor found. *Nature*, 453:80 – 83, 2008.

[7] W. Cai, F. Ellinger, R. Tetzlaff, and T. Schmidt. Abel dynamics of titanium dioxide memristor based on nonlinear ionic drift model. *arXiv preprint arXiv:1105.2668*, 2011.

[8] Z. Biolek, D. Biolek, and V. Biolkova. Analytical solution of circuits employing voltage- and current-excited memristors. *IEEE Transactions on Circuits and Systems I*, 59(11):2619 –2628, 2012.